To be submitted to *The Astrophysical Journal*

The Detection of Circumnuclear X-ray Emission from the Seyfert Galaxy NGC 3516

I.M. George[1,2], T.J. Turner[1,2], H. Netzer[3], S.B. Kraemer[4,5], J. Ruiz[4,5], D. Chelouche[3], D.M. Crenshaw[6], T. Yaqoob[2,7], K. Nandra[2,8], R.F. Mushotzky[2]

ABSTRACT

We present the first high-resolution, X-ray image of the circumnuclear regions of the Seyfert 1 galaxy NGC 3516, using the *Chandra X-ray Observatory* (*CXO*). All three of the *CXO* observations reported were performed with one of the two grating assemblies in place, and here we restrict our analysis to undispersed photons (i.e. those detected in the zeroth-order).

A previously-unknown X-ray source is detected ~6 arcsec ($1.1h_{75}^{-1}$ kpc) NNE of the nucleus (position angle ~29 degrees) which we designate CXOU 110648.1+723412. Its spectrum can be characterized as a power law with a photon index Γ ~1.8–2.6, or as thermal emission with a temperature kT ~0.7–3 keV. Assuming a location within NGC 3516, isotropic emission implies a luminosity L ~$2\text{–}8\times10^{39}h_{75}^{-2}$ erg s^{-1} in the 0.4–2 keV band. If due to

[1]Joint Center for Astrophysics, Department of Physics, University of Maryland, Baltimore County, 1000 Hilltop Circle, Baltimore, MD 21250

[2]Laboratory for High Energy Astrophysics, Code 662, NASA/Goddard Space Flight Center, Greenbelt, MD 20771

[3]School of Physics and Astronomy and the Wise Observatory, The Beverly and Raymond Sackler Faculty of Exact Sciences, Tel Aviv University, Tel Aviv 69978, Israel.

[4]Laboratory for Astronomy and Solar Physics, Code 681, NASA/Goddard Space Flight Center, Greenbelt, MD 20771

[5]Institute for Astrophysics and Computational Sciences, The Catholic University of America, Washington D.C. 20064

[6]Department of Physics and Astronomy, Georgia State University, Atlanta, GA 30303

[7]Department of Physics & Astronomy, Johns Hopkins University, 3400 North Charles Street, Baltimore, MD 21218

[8]Universities Space Research Association

a single point source, the object is super-Eddington for a $1.4M_{\odot}$ neutron star. However, multiple sources or a small, extended source cannot be excluded using the current data.

Large-scale extended X-ray emission is also detected out to $\sim$ 10 arcsec ($\sim 2h_{75}^{-1}$ kpc) from the nucleus to the NE and SW, and is approximately aligned with the morphologies of the radio emission and extended narrow emission line region (ENLR). The mean luminosity of this emission is $1\text{–}5\times10^{37}h_{75}^{-2}$ erg s^{-1} arcsec^{-2}, in the 0.4–2 keV band. Unfortunately the current data cannot usefully constrain its spectrum.

These results are consistent with earlier suggestions of circumnuclear X-ray emission in NGC 3516 based on *ROSAT* observations, and thus provide the first clear detection of extended X-ray emission in a Seyfert 1.0 galaxy. If the extended emission is due to scattering of the nuclear X-ray continuum, then the pressure in the X-ray emitting gas is at least two orders of magnitude too small to provide the confining medium for the ENLR clouds.

Subject headings: galaxies: active – galaxies: individual (NGC 3516) – galaxies: nuclei – galaxies: Seyfert – X-rays: galaxies

1. INTRODUCTION

NGC 3516 is an apparently undisturbed SB0 type, with the bar $\sim$25 arcsec long aligned N–S, plus a possible outer oval 30–100 arcsec with a major axis aligned in the NE–SW direction (e.g. Adams 1977). It is one of the "nebulae" included in the studies of Hubble (1926), and noted as having high-excitation emission lines by Seyfert (1943). The nucleus has since been shown to possess an archetypal Seyfert 1 spectrum (e.g. Khachikian & Weedman 1974), and since been studied extensively at all accessible wavebands from radio to X-rays (e.g. see Arribas et al 1997; Guainazzi, Marshall, Parmar 2001; and references therein).

Following Ferruit et al. (1998, and references therein), hereafter we adopt a distance of $35.7h_{75}^{-1}$ Mpc to the nucleus of NGC 3516 (where $h_{75} = H_0/75$ km s^{-1} Mpc^{-1}), thus 1 arcsec $\equiv 173h_{75}^{-1}$ pc. In the radio, an unresolved, flat-spectrum core centered on the optical nucleus has been known about since the first VLA surveys of Seyferts (e.g. Ulvestad & Wilson 1984). However, more recent, deeper maps at 20 and 6 cm have also revealed a series of "blobs" forming an elongated, curved structure extending out to $\sim$20 arcsec ($\sim 3.5h_{75}^{-1}$ kpc) to the NE (Baum et al. 1993; Miyaji, Wilson & Pérez-Fournon 1992). A much weaker, radio counter-structure to the SW of the nucleus has also been suggested (Wrobel & Heeschen 1988) but, as yet, has not been confirmed.

In the optical and UV, regions of line emission have been detected out to ~ 30 arcsec ($\sim 5.2h_{75}^{-1}$ kpc) from the nucleus, with an asymmetric (often called Z-shaped) morphology within the central 10 arcsec ($\sim 1.7h_{75}^{-1}$ kpc) – see Ferruit, Wilson, Mulchaey (1998), and references therein. The kinematic studies of this extended narrow emission line region (ENLR) show peculiar motions (e.g. Ulrich, Péquignot 1980) while the stellar velocity field appears normal (Arribas et al. 1997). It has been suggested that the morphology and kinematics of the ionized gas are the result of a bent, bipolar outflow from the nucleus or due to entrainment within a precessing radio jet (e.g. Veilleux, Tully, Bland-Hawthorn 1993; Ferruit et al. 1998).

X-ray emission from NGC 3516 was first detected in 1979 by the Imaging Proportional Counter on board the *Einstein Observatory* (e.g. Maccacaro, Garilli & Mereghetti 1987), and studied by all the major X-ray observatories since. The X-ray continuum exhibits spectral and temporal characteristics common to Seyfert 1 galaxies, including Fe Kα emission, absorption due to ionized gas (a "warm absorber") and an apparently variable power law continuum (e.g. Guainazzi et al 2001, and references therein). However, most relevant to the work discussed here, is the suggestion of extended emission in 0.1–2 keV band in data obtained using the High Resolution Imager (HRI) on board *ROSAT*. Morse et al. (1995) found an elongation in X-ray emission on scales 10–30 arcsec (2–$5h_{75}^{-1}$ kpc) approximately aligned with ENLR described above. However, as noted by Morse et al., this elongation could be the result of residual errors in the spacecraft aspect solution. The morphology of any extended X-ray emission within 10 arcsec could not be studied in these HRI data since any such emission was swamped by the instrumentally-scattered emission from the nucleus.

Here we present new X-ray data from NGC 3516 obtained with high spatial-resolution using the *Chandra X-ray Observatory* (*CXO*). We restrict our discussion to the non-nuclear emission. The results from the nuclear emission is presented in Netzer et al. (2001) and Turner et al. (in preparation). In §2 we describe the observations, and in §3 the basic results from our spatial analysis. The characteristics of an off-nuclear source are described in §4, and those of the extended X-ray emission in §5. We discuss our findings and present our conclusions in §6. Throughout we assume a Galactic column density of $N_{HI}^{gal} = 2.9\times10^{20}$ cm^{-2} appropriate for this line of sight (Murphy et al 1996).

2. THE OBSERVATIONS & DATA REDUCTION

The data from NGC 3516 reported here were obtained from three observations using the *CXO*: a 47 ks observation in 2000 September, and two observations (of approximately 40 ks and 75 ks respectively) in 2001 April (see Table 1). All observations were performed with the "S-array" of the Advanced CCD Imaging Spectrometer (ACIS: e.g. Nousek et al 1998)

in the focal plane (with a temperature of $-120°$ C). The Low Energy Transmission Grating Spectrometer (LETGS: e.g. Brinkman et al. 1997) was in the optical path during the earlier observation, while the High Energy Transmission Grating Spectrometer (HETGS: e.g. Markert et al. 1994) was in place during the latter observations. In all cases, the zeroth-order image of the nucleus of NGC 3516 was close to the optical axis of the telescope and fell on the (back-illuminated) ACIS-S3 chip. Here we restrict our analysis to the non-nuclear emission detected using the zeroth-order from the respective gratings. The results from the nucleus of NGC 3516 are discussed in Netzer et al. (2001) and Turner et al. (in preparation).

For completeness, we review a number of general characteristics associated with the configuration of the telescope and detector. Firstly, the ACIS pixels are 0.492 arcsec on a side ($85h_{75}^{-1}$ kpc at the assumed distance to NGC 3516). The X-ray telescope has a FWHM of 0.84 arcsec at energies $\lesssim 6$ keV (the presence of neither the LETGS nor the HETGS in the optical path is thought to degrade this significantly). Thus the zeroth-order image of bright sources will be "piled-up"[9] in their central pixel(s), and hence exhibit an artificial deficit of photons in the central pixel(s). Secondly, the images of bright sources will also exhibit a read-out stripe[10]. Thirdly, with the gratings in the optical path, the dispersed (1^{st}–, 2^{nd}–, 3^{rd}–order etc.) spectra will be projected onto the plane of the sky. For example, in the 1^{st}–order, the LETGS still has significant effective area (~ 1 cm^{-2}) at 9 keV. Such photons will appear $\simeq$29 arcsec from the zeroth–order image.

In all subsequent analysis, the above effects have been taken into account as follows. We ignore all events detected within 1 arcsec (approximately 2 ACIS pixels) of the position expected (and detected) due to the zeroth–order position of the target source (i.e, the nucleus of NGC 3516). "Pile-up" is of negligible concern here since we do not discuss the nuclear emission. In addition, on an observation-by-observation basis, we give zero-weight to all events within ± 1 pixel of the read-out stripe. Finally, outside a radius 25 arcsec we give zero-weight to all events within a polar angle ± 8 degrees of the location of the dispersed spectra.

The data analysis was performed using the *Chandra* `CALDB` (v2.7), and the `CIAO` (v2.0.3)

---

[9]This is the result of more than one incident photon depositing its energy in a given pixel within a single CCD frame. The charge clouds from the individual photons will be combined and hence interpreted by the on-board electronics as due to a single "event" by an incident photon of higher energy.

[10]The read-out stripe is due to events being detected by the CCDs while the image frame is being read out. These "out-of-time" events are recorded at an incorrect row in the CCD, and in the (RA,dec) coordinate system used here, will result in a stripe at an angle equal to the roll angle of the spacecraft.

and `HEAsoft` (v5.1) software packages. Standard data reduction procedures were followed, including the removal of the "streaks" from the ACIS CCDs (using `destreak` v 1.3; Houck 2000), the selection of events with well-understood "grades"[11], and the correction of a known error in the aspect solution for the first observation.

3. SPATIAL ANALYSIS

A bright point-like source is clearly evident in each observation consistent (within the uncertainties of the *CXO* aspect reconstruction) with the position of the nucleus of NGC 3516 (RA=11h 06m 47.490s, dec=+72d 34m 06.88s, with a 95% confidence radius of 0.25s; Clements 1981). The residual errors in the aspect solutions (see Table 1) were corrected manually, and the events then re-projected onto a common tangent-plane projection (centered on the optical nucleus).

In the upper panels of Fig. 1 we show the images of the circumnuclear region in the 0.2–1 keV and 4–8 keV bands. The soft band image reveals an off-nuclear source ~6 arcsec ($\sim 1.1 h_{75}^{-1}$ kpc) to the NNE (position angle ~29 degrees) of the nucleus of NGC 3516, and extended emission in the NE–SW direction stretching out to approximately 10 arcsec ($\sim 2 h_{75}^{-1}$ kpc) from the nucleus. At high energies only the nucleus of NGC 3516 is detected, illustrating that neither the extended emission nor the off-nuclear source are obvious artifacts of the *CXO* aspect reconstruction.

In the lower panels of Fig. 1 we show the corresponding radial point spread functions (rpsfs) from the NE and SW quadrants. For comparison also shown (the black histograms) are corresponding rpsfs from the two archival HETGS observations of the bright quasar 3C 273 currently available to us, superimposed on the the ambient background. (The known X-ray jet in 3C 273 was excluded from the calculation.) In the 0.2–1 keV band, excess emission is clearly seen in NGC 3516 in both the NE and SW quadrants at radii ~3–10 arcsec (~0.5–1.7 h_{75}^{-1} kpc). The spike in the rpsf of the NE quadrant at ~6 arcsec is due to off-nuclear source. In contrast, the rpsf in the 4–8 keV band are consistent with the instrumental profile (right panel of Fig. 1).

---

[11]Each photon detected is assigned a "grade" based on the distribution of the charge deposited within a 3 × 3 array of CCD pixels. Only grades equivalent to "*ASCA* grades" 0, 2, 3, 4 and 6 are used here.

3.1. Extraction Regions

For the subsequent analysis we make use of data extracted using the following regions. The first region is a circle of radius 1.8 arcsec centered on the off-nuclear source (ie. equivalent to 42 ACIS pixels). Hereafter we refer to this region as the "off-nuclear source cell". The second region encompasses the extended emission, namely the NE and SW quadrant of an annulus stretching from 3–10 arcsec from the nucleus of NGC 3516 (excluding the region around the off-nuclear source). This region encompasses 290 ACIS pixels, and hereafter we refer to it as the "extended cell". The third region is used as a background region and consists of the NE and SW quadrant of an annulus stretching from 10-20 arcsec from the nucleus. This region encompasses 1545 ACIS pixels, and hereafter refered to as the "background cell".

In Fig.2 we show the counts spectra *per pixel* from each of these regions. It should be noted that due to the different transmission characteristics of the LETGS and HETGS, the effective area is different for each grating/detector combinations. These are shown in the lower panels of Fig.2, and necessitate separate spectral analysis of the two datasets.

4. THE OFF-NUCLEAR SOURCE CXOU 110648.1+723412

Astrometry using the position of the optical nucleus of NGC 3516 gives a location of the off-nuclear source at (J2000) RA=11h 06m 48.1s, dec=+72d 34m 12.5s, with an uncertainty of ∼1 arcsec. To the best of our knowledge, this is the first clear detection of a distinct source at this location and we designate it CXOU 110648.1+723412.

In the LETGS data set a total of 57 counts were detected in the 0.2–8 keV band from the off-nuclear source cell. A total of 114 counts were detected in this band from this cell in the HETGS data set. The ambient backgrounds in this band, derived using the extended cell (renormalising by the ratios of the areas of the cells) are 8 counts in the LETGS and 20 counts in the HETGS data sets.

As illustrated in Fig.2, CXOU 110648.1+723412 is significantly detected in the ∼0.3–4 keV band in both the LETGS and HETGS data sets. However, with so few net counts, clearly only limited temporal and spectral information is available. We have grouped the spectra such that each new bin contained at least 20 counts, hence allowing an analysis using χ^2-statistics. This resulted in only 2 bins for the LETGS data set, and 5 bins for the HETGS data set. We find the spectra at all epochs to be consistent with a simple power-law continuum, a thermal bremsstrahlung continuum, or emission from a collisionally ionized plasma. For the power-law continuum, for which we obtain a best-fit with a reduced χ^2-statistic, $\chi^2_\nu = 1.90$ for 5 degrees of freedom (dof), the 90% confidence ranges for the photon

index (Γ), flux and luminosity in the 0.4–2 keV band (the latter after correcting for N_{HI}^{gal}, assuming isotropic emission and a location within NGC 3516) are $1.8 \lesssim \Gamma \lesssim 2.6$, f(0.4-2 keV) $\simeq$ 2.1–3.4 $\times 10^{-14}$ erg cm^{-2} s^{-1}, and L(0.4-2 keV) $\simeq$ 3.7–5.9 $\times 10^{39} h_{75}^{-2}$ erg s^{-1}. For the thermal bremsstrahlung continuum ($\chi_\nu^2/dof = 1.99/5$), we find the temperature in the range $0.9 \lesssim kT$(keV)$\lesssim 3.3$, f(0.4-2 keV) $\simeq$ 1.8–4.3 $\times 10^{-14}$ erg cm^{-2} s^{-1}, and L(0.4-2 keV) $\simeq$ 3.2–7.5 $\times 10^{39} h_{75}^{-2}$ erg s^{-1}. For a collisionally ionized plasma ($\chi_\nu^2/dof = 2.24/4$), we require the abundance of all elements to be $\lesssim$ 63% of their cosmic values, the temperature in the range $0.7 \lesssim kT$(keV)$\lesssim 3.1$, f(0.4-2 keV) $\simeq$ 1.4–4.8 $\times 10^{-14}$ erg cm^{-2} s^{-1}, and L(0.4-2 keV) $\simeq$ 2.4–8.3 $\times 10^{39} h_{75}^{-2}$ erg s^{-1}. For these models, we find no requirement for absorption in excess of N_{HI}^{gal}, although the constraints that can be placed on any such component are poor (typically $\lesssim$few$\times 10^{21}$ cm^{-2}). For future reference, at 90% confidence we find an upper limit of the flux in the 4–8 keV band of 4×10^{-14} erg cm^{-2} s^{-1}.

It should be noted that the above results do not change significantly if the background from the background cell is used instead of that from the extended cell. Such an approach would be more appropriate if the emission from within the extended cell was the result of a relatively few faint, discrete sources rather than truly-uniform, extended emission.

It is possible that CXOU 110648.1+723412 is extended. Indeed our spatial analysis reveals evidence for some extension on a scale $\sim$0.5 arcsec ($\sim 0.2 h_{75}^{-1}$ kpc). However given the co-addition of several observations, and the likely presence of (probably patchy) underlying extended emission, further observations are required to investigate this possibility.

5. THE EXTENDED EMISSION

The region used to extract the extended emission consists of 290 ACIS pixels (70.2 arcsec^2) in the NE and SW quadrant of an annulus stretching from 3–10 arcsec from the nucleus of NGC 3516 (excluding the region around CXOU 110648.1+723412). Unfortunately there are insufficient counts per pixel to determine whether the X-ray emission from this region is smooth, patchy, and/or due to a relatively small number of discrete sources. Thus below we discuss the "mean" X-ray characteristics of this region.

Totals of 55 and 141 counts were detected in the 0.2–8 keV band from this region in the LETGS and HETGS data sets (respectively). Renormalising for the areas, from the background cell we estimate ambient backgrounds of 29 and 76 counts in the extended cell (respectively). As illustrated in Fig.2, extended emission is significantly detected in the $\sim$0.3–4 keV band in the LETGS data set, and at most energies in the $\sim$0.3–6 keV band in the HETGS data set. However, as for CXOU 110648.1+723412, there are again clearly too

few net counts for detailed temporal or spectral analysis. Grouping the spectra such that each new bin contained at least 20 counts results in 2 bins for the LETGS data set, and 7 bins for the HETGS data set. We find the spectra to be formally consistent with a power law continuum ($\chi^2_\nu/dof = 0.83/7$), with 90% confidence ranges of $0.6 \lesssim \Gamma \lesssim 2.8$, f(0.4-2 keV) $\simeq 0.4$–1.8×10^{-14} erg cm^{-2} s^{-1}, and L(0.4-2 keV) $\simeq 0.8$–$3.1 \times 10^{39} h_{75}^{-2}$ erg s^{-1}. A thermal bremsstrahlung continuum is also acceptable ($\chi^2_\nu/dof = 0.97/7$), with kT(keV)$\gtrsim 1.3$, f(0.4-2 keV) $\simeq 0.5$–2.0×10^{-14} erg cm^{-2} s^{-1}, (0.7–2.8×10^{-16} erg cm^{-2} s^{-1} arcsec^{-2}), and L(0.4-2 keV) $\simeq 0.8$–$3.3 \times 10^{39} h_{75}^{-2}$ erg s^{-1} (1.1–$4.8 \times 10^{37} h_{75}^{-2}$ erg s^{-1} arcsec^{-2}). Clearly a number of more complex spectral forms are also consistent with the data. We find no requirement for absorption in excess of N_{HI}^{gal}, although again the constraints that are placed on any such component are poor with the current data ($\lesssim$few$\times 10^{21}$ cm^{-2}). The current data have too low a signal-to-noise ratio to determine whether the spectra from the NE and SW quadrants differ (e.g. whether they suffer different amounts of intrinsic absorption as might be expected if they lie on different sides of the galactic plane). As for CXOU 110648.1+723412, at 90% confidence the upper limit of the flux in the 4–8 keV band is 4×10^{-14} erg cm^{-2} s^{-1}.

6. DISCUSSION & CONCLUSIONS

The spatial resolution of *CXO* finally allows the innermost regions ($\lesssim$1 kpc) of the nearest galaxies to be probed in X-rays. Already observations have shown that besides point sources (many of which appear to be emitting at super-Eddington luminosities), a large fraction of galaxies have extended X-ray emission on scales ~0.5–1.5 kpc (see Weaver 2001 for a recent review). Furthermore, this extended X-ray emission often has an anisotropic morphology, and is aligned with other anisotropic structures such as the radio emission and/or ENLR.

The data presented here show that NGC 3516 fits into this picture. We have found a distinct off-nuclear source (CXOU 110648.1+723412) which is embedded within the extended X-ray emission $\sim$ 6 arcsec ($1.1 h_{75}^{-1}$ kpc) NNE of the nucleus. More interestingly, we have found extended X-ray emission in the ~0.3–4 keV band, detected out to a radius $\sim$ 10 arcsec ($\sim 2 h_{75}^{-1}$ kpc) from the nucleus. The extended emission appears to be anisotropically distributed in the NE–SW direction, although instrumental artifacts (most notably the read-out streak associated with the relatively-bright nuclear emission) prevent us from being certain. However we do note that an elongation in this direction was suggested by Morse et al. (1995) based on *ROSAT* HRI data. In the left panel of Fig. 3 we show the circumnuclear regions of NGC 3516 in the optical band, obtained from an archival *HST*/WFPC2 observation using the linear ramp filter (FR533N) centered on the red-shifted [OIII] (5007Å) emission line. As shown previously by Ferruit et al. (1998), the morphology of the [OIII] emission is complex,

but shows a distinct anisotropy in the NE–SW direction. The right panel of Fig. 3 compares the [OIII] and soft X-ray morphologies. Clearly there appears to be good agreement between the alignments.

6.1. The Off-nuclear source

The source CXOU 110648.1+723412 is highly likely to be located within the galaxy NGC 3516. The density of background active galactic nuclei (AGN) at this flux level in the 0.5–2 keV band is $\sim$ 20 per square degree (e.g. Hasinger et al. 1998), thus the probability of a background source within 6 arcsec of the nucleus of NGC 3516 is $\sim 2 \times 10^{-4}$. Similarly the probability that the emission is due to a foreground (Galactic) source is at least a factor 2 lower (e.g. Kuntz & Snowden 2001).

As stated in §4, based on the data currently available we cannot determine unambiguously whether CXOU 110648.1+723412 is a true point-source, or a relatively small, but diffuse, enhancement in the extended emission. If it is a point-source, indeed located in NGC 3516 and emitting isotropically, then its X-ray luminosity ($L(0.4-2\ keV)$ $\sim$2–$8\times10^{39}h_{75}^{-2}$ erg s^{-1}) is above the Eddington luminosity for a $1.4M_{\odot}$ neutron star. Such "super-luminous" off-nuclear sources are being regularly found by *CXO* (e.g. Griffiths et al. 2000; Fabbiano, Zezas, Murray 2001; George et al 2001; Pence et al 2001) with similar spectral characteristics as CXOU 110648.1+723412. Alternatively, CXOU 110648.1+723412 could be the result of the superposition of several sub-Eddington sources, or simply a local enhancement within the diffuse emission. Higher quality X-ray spectra and temporal studies are required to distinguish between these possibilities.

Interestingly, as can be seen from the right panel of Fig. 3, CXOU 110648.1+723412 is located just N of the [OIII] E–W linear structure to the NE of the nucleus. The lack of [OIII] emission in the immediate vicinity of the X-ray source may be the result of its radiation field photo-ionizing oxygen to OIV and higher.

6.2. The Extended X-ray Emission

There are several possible origins for the extended X-ray emission reported here. Clearly it might not be truly extended emission at all, instead being the result (at least in part) of a relatively-small number of faint, discrete sources. Certainly we see one clear discrete source, CXOU 110648.1+723412, and there are some indications of patchiness within the rest of the extended emission. The current *CXO* data simply do not have sufficient signal-to-noise to

usefully constrain the possibility. Nevertheless, if the observed X-ray emission is (primarily) extended, then it may be the result of i) emission from hot, collisionally-ionized gas, and/or ii) emission by gas photo-ionized by the intense nuclear radiation field. The former may be related to the presence of active star-forming regions. The latter will include the scattering of the nuclear radiation field. Both situations could exist within all/some of the region, and at least some of the gas could be under the influence of both collisional- and photo-ionization processes. In principle the dominant ionization mechanism can be determined from a detailed study of the X-ray spectrum. Unfortunately the current *CXO* data simply do not have sufficient signal-to-noise.

Diffuse emission in the 0.4–2 keV band, with a luminosity $\lesssim$few$\times 10^{39}$ erg s^{-1}, has been detected from the inner few kpc of a number of galaxies. These include both "classic" AGN (e.g. the Seyfert 1.5 galaxy NGC 4151; Ogle et al. 2000, and the Seyfert 2 galaxies Circinus and NGC 1068; Sambruna et al. 2001; Young, Wilson, Shopbell 2001), those with low-luminosity AGN (e.g. M51; Terashima & Wilson 2001), and "normal" galaxies (e.g. the starburst galaxy M82; Grifffiths et al. 2000, and nearby spiral M81; Tennant et al. 2001). Thus it is not clear how (if at all) the diffuse X-ray emission in NGC 3516 might be related to the presence of an active nucleus. Nevertheless it is of interest to explore the case where the extended emission arises solely from electron-scattering of the nuclear radiation field.

Let us adopt a conical geometry with a half-opening angle, β, extending to a radius R. Within these cones, we assume that the electrons are distributed in clouds, the latter having with a volume filling factor, f_V. Let L_{pri} be the mean (time-averaged) luminosity of the nuclear source. If we assume neither the electron density, n_e, within the clouds nor f_V changes with radius, and that there is negligible attenuation of the photons en route, then $f_V n_e = L_{scat}/(L_{pri} \cos\beta \sigma_{\rm T} R)$, where L_{scat} is the luminosity of the scattered radiation, and σ_T the Thomson cross-section. Thus for R =2 kpc and β =45 degrees, $f_V n_e = \simeq 100\ L_{scat}/L_{pri}$ cm^{-3}. The spectrum and luminosity of nucleus in the 7×10^3 years prior to the photons leaving NGC 3516 is of course unknown. However as discussed in Netzer et al. (2002), there is evidence from X-ray observations over the past decade that the *emitted* spectrum has not changed in shape and is consistent with a power law of photon index $\Gamma = 1.9$. Thus we adopt such a form. Significant changes in the luminosity of the nucleus have been observed (by a factor $\sim$10). Here we simply assume the approximate average luminosity of the observations make to date, namely L_{pri}(0.4–2 keV) $\simeq 4 \times 10^{42} h_{75}^{-2}$ erg s^{-1}. From §5, L_{scat}(0.4–2 keV) $\simeq 2 \times 10^{39} h_{75}^{-2}$ erg s^{-1} for such a spectral form. Hence $f_V n_e \simeq 0.05$ cm^{-3}, and the total mass out to a radius of 2 kpc is $\sim 2 \times 10^7 M_\odot$. Such a model is consistent with the lack of extended emission detected at high energies. Our adopted nuclear spectrum has L_{pri}(4–8 keV) $\simeq 2 \times 10^{42} h_{75}^{-2}$ erg s^{-1}. Thus we predict L_{scat}(4–8 keV) $\simeq 10^{39} h_{75}^{-2}$ erg s^{-1}, and hence a flux in this band ($\simeq 7 \times 10^{-15}$ erg cm^{-2} s^{-1}) easily within the observed upper limit

reported in §5.

Using an ionization parameter defined as $U_{ox} = Q/4\pi r^2 n_e c$, where Q is the number of photons emitted per second in the 0.538–10 keV band. Our adopted nuclear spectrum implies $U_{ox} \simeq 0.02 f_V r_{kpc}^{-2}$ at a radius r_{kpc} kpc, and a column density (integrated along the cone) $N_{\rm H} \simeq 1.6 \times 10^{20} r_{kpc}$ cm^2. Unless $f_V \lesssim 10^{-2}$, this combination of U_{ox} and $N_{\rm H}$ imply the gas is indeed highly ionized out to a radius of at least several kpc, and hence our assumptions are valid. The strongest spectral features emitted by such gas are likely to be CVI, OVII, OVIII, and NeIX recombination continua and emission lines. We note that similar features have been observed in X-ray spectra of Seyfert 2 galaxies (e.g., NGC 1068; Young, Wilson, & Shopbell 2001).

Under the above assumptions, the extended gas has a significantly smaller column density than the "warm-absorbers" seen in Seyfert 1 galaxies (typically 10^{21}–10^{23} cm^2, e.g. George et al. 1998). Indeed, Netzer et al (2002) have shown that the warm-absorber in NGC 3516 has a column density $\sim 10^{22}$ cm^2, a density $n_e \gtrsim$few$\times 10^6$ cm^{-3}, and is located at a radius $r \lesssim$0.5 pc from the nucleus. Thus these data do not support the idea that the gas responsible for the warm absorbers seen in Seyfert 1 galaxies is the same gas that is seen in emission in Seyfert 2 galaxies.

Finally we note that under the assumption that the extended X-ray emitting gas is indeed photo-ionized, then for $f_V \simeq 1$ its temperature is $T \simeq 10^5$ K. Thus $n_e T \sim$ few$\times 10^3$ cm^{-3} K. As implicit from §1, the extended X-ray emitting gas appears to be co-spatial with the ENLR in NGC 3516 (see also Fig. 3). Photo-ionization models of the optical line ratios observed from gas responsible for the ENLR give $n_e T \lesssim$few $\times 10^5$– few $\times 10^6$ cm^{-3} K (e.g. Ulrich & Péquignot 1980; Aoki et al. 1994). Hence the pressure ratio between the gas responsible for the extended X-ray emission and ENLR is $\lesssim 10^{-2}$. The two are not in pressure equilibrium so the X-ray emitting gas cannot be the confining medium for the ENLR clouds. Such a situation has also been found in the case of NGC 4151 (Ogle et al. 2000). There may well be other effects such as a dynamical interaction between these two gaseous components, but an exploration of this is beyond the scope of the current paper.

We thank Keith Arnaud for providing some of the software used for this project. We acknowledge the financial support of the Joint Center for Astrophysics (IMG, TJT), NASA (TJT, through grant number NAG5-7385), and the Universities Space Research Association (KN). This research has made use of the Simbad database, operated by the Centre de Données astronimiques de Strasbourg (CDS); the `VizieR` Service for Astronomical Catalogues, developed by CDS and ESA/ESRIN; the NASA/IPAC Extragalactic Database (NED), operated by the Jet Propulsion Laboratory, California Institute of Technology, under

contract with NASA; and of data obtained through the HEASARC on-line service, provided by NASA/GSFC.

REFERENCES

Adams, T.F., 1977, ApJS, 33, 19

Aoki, K., Ohtani, H., Yoshida, M., Kosugi, G., 1994, PASJ, 46, 539

Arribas, A., Mediavilla, E., Garćia-Lorenzo, B., Del Burgo, C., 1997, ApJ, 490, 227

Baum, S.A., O'Dea, C.P., Dallacassa, D., De Brruyn, A.G., Pedlar, A., 1993, ApJ, 419, 553

Brinkman, A.C., et al. 1997, Proc. SPIE, 3113, 181

Clements, E.D. 1981, MNRAS, 197, 829

Fabbiano, G., Zezas, A., Murray, S.S., 2001, ApJ, 554, 1035

Ferruit, P., Wilson, A.S., Mulchaey, J.S. 1998, ApJ, 509, 646

George, I.M., Turner, T.J., Netzer, H., Nandra, K., Mushotzky, R.F, Yaqoob, T., 1998, ApJS, 114, 73

George, I.M., Mushotzky, R.F, Yaqoob, T., Turner, T.J., Kraemer, S.B., Ptak, A.F., Nandra, K., Crenshaw, D.M., Netzer, H., 2001, ApJ, 559, 167

Griffiths, R.E., Ptak, A., Feigelson, E.D., Garmire, G., Townsley, L., Brandt, W.N., Sambruna, R., Bregman, J.N., 2000, Science, 290, 1325

Guainazzi, M., Marshall, W., Parmar, A.N., 2001, MNRAS, 323, 75

Hasinger, G., Burg, R., Giacconi, R., Schmidt, M., Trümper, J., Zamorani, G., 1998, A&A, 329, 482

Houck, J., 2000, MIT Center for Space Research Memorandum, 2000 Aug 01

Hubble, E., 1926, ApJ, 64, 321

Khachikian, E.Y., Weedman, D.W., 1974, ApJ, 192, 581

Kuntz, K.,D., Snowden, S.L., 2001, ApJ, 554, 684

Maccacaro, T., Garilli, B. & Mereghetti, S., 1987, AJ, 93, 1484

Markert, T. H., Canizares, C. R., Dewey, D., McGuirk, M., Pak, C. S., Schattenburg, M. L. 1994, Proc. SPIE, 2280, 168

Miyaji, T., Wilson, A.S., Pérez-Fournon, I., 1992, ApJ, 385, 137

Morse, J.A., Wilson, A.S., Elvis, M., Weaver, K.A., 1995, ApJ, 439,121

Murphy, E.M., Lockman, F.J., Laor, A., Elvis, M. 1996, ApJS, 105, 369

Netzer, H., Chelouche, D., George, I.M., Turner, T.J., Crenshaw, M., Kraemer, S., Nandra, K., 2002, ApJ, submitted

Nousek, J.A., et al. 1998, Proc. SPIE, 3444, 225

Ogle, P.M., Marshall, H.L., Lee, J.C., Canizares, C.R., 2000, ApJ, 545, L81

Pence, W.D., Snowden, S.L., Mukai, K., Kuntz, K.D., 2001, ApJ, in press

Sambruna, R.M., Brandt, W.N., Chartas, G., Netzer, H., Kaspi, S., Garmire, G.P., Nousek, J.A., Weaver, K.A., 2001, ApJ, 546, L9

Seyfert, C.K., 1943, ApJ, 97, 28

Tennant, A.F., Wu, K., Ghosh, K.K., Kolodziejczak, J.J., Swartz, D.A., 2001, ApJ, 549, L43

Terashima, Y., Wilson, A.S., 2001, ApJ, 560, 139

Ulrich, M.H., Péquignot, D., 1980, ApJ, 238, 45

Ulvestad, J.S., Wilson, A.S., 1984, ApJ, 285, 439

Veilleux, S., Tully, R.B., Bland-Hawthorn, J., 1993, AJ, 105, 1318

Weaver, K.A., 2001, in The Central Kiloparsec of Starburst and AGN: The La Palma Connection, eds. J.H. Knappen, J.E. Backman, I. Shlosman, T.J. Mahoney, ASP Conf. Series, in press

Wrobel, J.M., Heeschen, D.S., 1988, ApJ, 335, 677

Young, A.J., Wilson, A.S., Shopbell, P.L., 2001, ApJ, in press

---

This preprint was prepared with the AAS LaTeX macros v5.0.

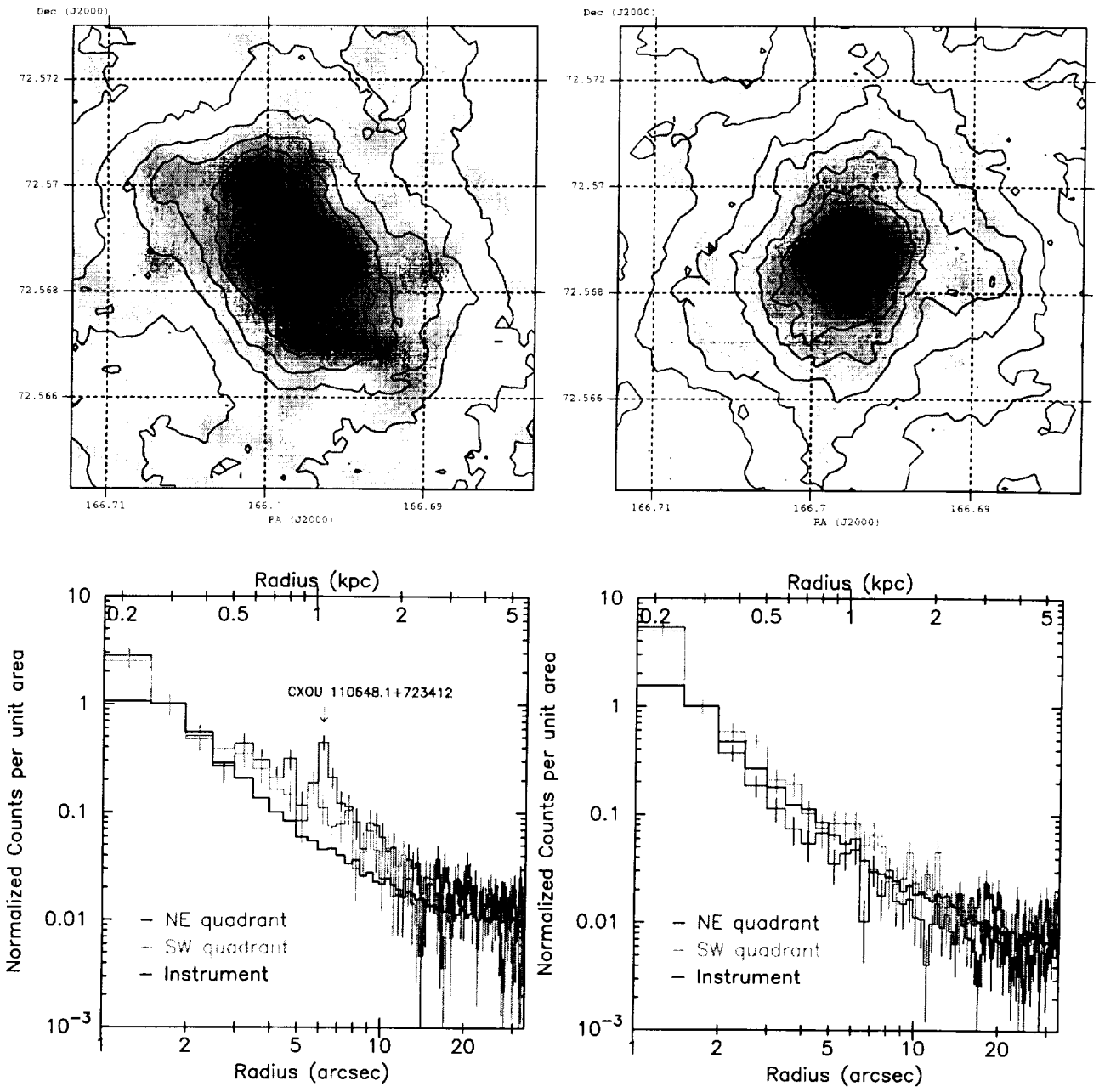

Fig. 1.— *Upper panels:* The central regions of NGC 3516 in the (left) 0.2–1 keV and (right) 4–8 keV bands. Each image is 64 × 64 pixels centered on the optical nucleus, with pixels 0.492 arcsec on a side (corresponding to approximately $85h_{75}^{-1}$ pc in NGC 3516). For clarity the image has been smoothed with a Gaussian with σ =3 pixels. The contours are derived from an adaptively smoothed version of the raw image. *Lower panels:* The corresponding radial point spread functions (rpsf) from the NE (red) and SW (green) quadrants. The black histograms show the rpsf derived from the observations of 3C 273 (see text), and hence taken to represent that of the instrument.

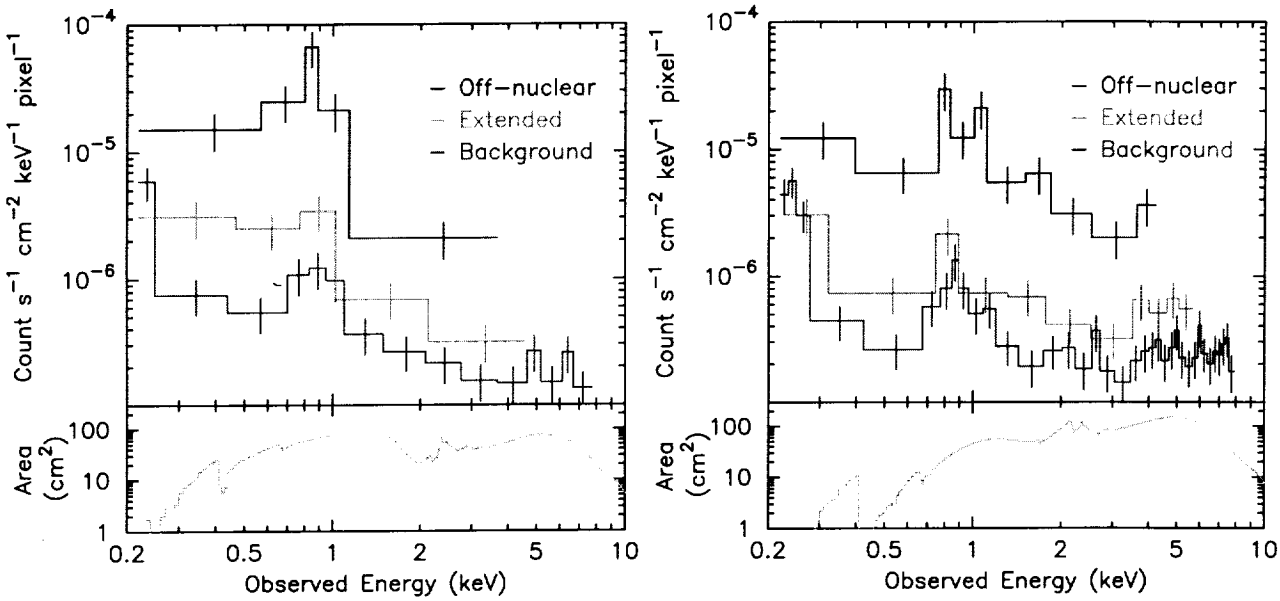

Fig. 2.— The spectra from three regions described in §3.1 derived from the LETGS (left) and HETGS (right). That from the off-nuclear source cell is shown in blue, the extended cell in green, and the background cell in red. In each case the spectra are shown *per pixel*, and have been rebinned such that each bin contains at least 10 counts. The lower panels show the effective area of each mirror/grating/detector combination.

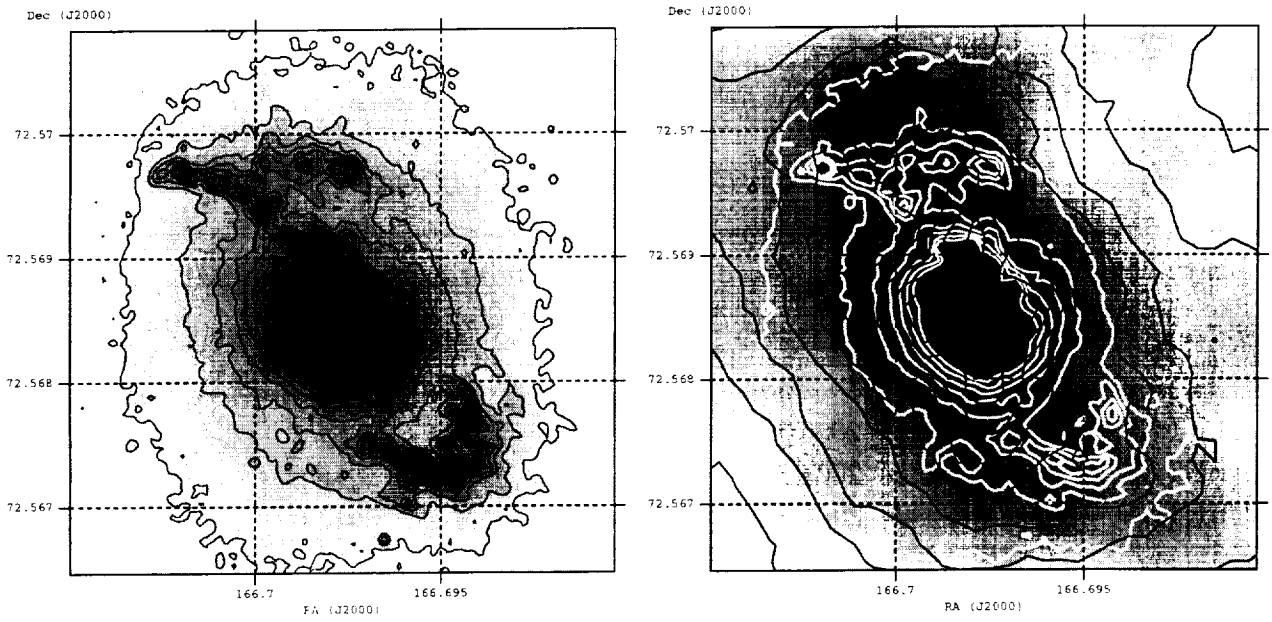

Fig. 3.— *Left: HST*/WFPC2 image of the circumnuclear regions of NGC 3516 in [OIII] (5007Å). The image is 15.7 arcsec on a side, corresponding to $2.73h_{75}^{-1}$ kpc at the distance of NGC 3516. Linearly-spaced contours are overlaid to illustrate the structures to the NE and SW of the nucleus. *Right:* The inner regions of the 0.2–1 keV image from Fig. 1 with the morphology of the [OIII] emission shown by the white contours (only every other contour is plotted for clarity).

Table 1. *CXO* OBSERVING LOG

Instrument	Seq./Obs.id.	Start Time (UTC)	Duration (ks)	Roll[a] (degrees)	ΔRA cos(dec)[b] (arcsec)	Δdec[b] (arcsec)
(1)	(2)	(3)	(4)	(5)	(6)	(7)
LETGS	700136/0831	2000 Sep 30 21:05:22	47.0	21.3	+0.51	+0.34
HETGS	700270/2431	2001 Apr 09 14:12:05	39.9	213.0	−0.41	+0.26
HETGS	700270/2080	2001 Apr 10 17:55:54	75.4	213.0	−0.43	+0.23

Note. — (*a*) spacecraft roll angle, measured from North towards West; (*b*) X-ray position minus optical position (RA=11h 06m 47.490s, dec=+72d 34m 06.88s; Clements 1981).